Fanar M. Abed[1], Luma K. Jasim[2], Marwa M. Bori[3]

Error Analysis of
Stonex X300 Laser Scanner Close-range Measurements

Abstract: This research reports an error analysis of close-range measurements from a Stonex X300 laser scanner in order to address range uncertainty behavior based on indoor experiments under fixed environmental conditions. The analysis includes procedures for estimating the precision and accuracy of the observational errors estimated from the Stonex X300 observations and conducted at intervals of 5 m within a range of 5 to 30 m. The laser 3D point cloud data of the individual scans is analyzed following a roughness analysis prior to the implementation of a Levenberg–Marquardt iterative closest points (LM-ICP) registration. This leads to identifying the level of roughness that was encountered due to the range-finder's limitations in close-ranging as well as measurements that were obtained from extreme incident angle signals. The measurements were processed using a statistical outlier removal (SOR) filter to reduce the noise impact toward a smoother data set. The geometric differences and the RMSE values in the 3D coordinate directions were computed and analyzed, which showed the potential of the Stonex X300 measurements in close-ranging following a careful statistical analysis. It was found that the error differences in the vertical direction had a consistent behavior when the range increased, whereas the errors in the horizontal direction varied. However, it is more common to produce errors in the vertical direction as compared to the horizontal one.

Keywords: terrestrial laser scanning, Stonex X300, close-range measurements, error analysis, accuracy assessment, range uncertainty

---

[1] University of Baghdad, College of Engineering, Department of Surveying Engineering, Baghdad, Iraq, email: fanar.mansour@coeng.uobaghdad.edu.iq (corresponding author),
    https://orcid.org/0000-0002-0919-5161

[2] University of Baghdad, College of Engineering, Department of Surveying Engineering, Baghdad, Iraq, email: luma.k@coeng.uobaghdad.edu.iq, https://orcid.org/0000-0003-2813-8856

[3] University of Baghdad, College of Engineering, Department of Surveying Engineering, Baghdad, Iraq, email: marwah.m@coeng.uobaghdad.edu.iq

1.   Introduction

Static scanners are generally classified into three main systems according to the range-finder type and scanning technology: time of flight (TOF), phase shift, and triangulation-based systems [1–3]. TOF systems are designed to work in mid-range and long-range environments to provide accurate results [3–5]. The accuracy of their laser measurements depends on the system type, scan configuration, scan object properties, and environmental conditions [6, 7]. This accuracy of the range measurements is reduced as the range increases in most TOF systems [8]. However, close-range measurements still encounter a certain level of uncertainty due to different error sources (i.e., instrumental, object-related, environmental, and methodological errors) [9]. This level of uncertainty is significantly increased as the scanner approaches its minimum scan range [1, 3, 9].

In TOF devices, modeling errors in close-ranging are applied in order to check the signal-to-noise impact and evaluate the performance in order to investigate the effect of the range uncertainty of the terrestrial laser scanning (TLS) measurements. This can be achieved by applying an error model to accumulate the systematic errors that are delivered from these measurements. As laser devices record the range, horizontal angle, and vertical (zenith) angle of individual surface points in a scene, the following generic error model can be considered [10]:

$$r_c = f_r(r_m, \theta_m, \varphi_m, p_1, p_2, \ldots, p_q) \tag{1}$$

$$\theta_c = f_\theta(r_m, \theta_m, \varphi_m, p_1, p_2, \ldots, p_q) \tag{2}$$

$$\varphi_c = f_\varphi(r_m, \theta_m, \varphi_m, p_1, p_2, \ldots, p_q) \tag{3}$$

where r_c, θ_c, φ_c represent the corrected range, horizontal angle, and vertical angle, respectively, r_m, θ_m, φ_m represent the measured range, horizontal angle, and vertical angle, respectively, p_i ($i = 1, \ldots, q$) represents the misalignment parameters (e.g., collimation error, transit tilt, encoder eccentricity, etc.), and f_r, f_θ, f_φ are functions that define the relationships between each measured and corrected value.

Ranging errors in TLS systems have been discussed in several studies [9–13]. However, establishing an absolute performance routine that fits with the majority of TOF devices is a challenging task, as numerous manufacturers of TLS systems are available today; each system has a specific error model that is based on its manufacturing specification. Ranging errors in TLS were reported by [14] using an EDM baseline-calibration approach. The authors mounted low-cost targets on five individual pillars that were located on a 600-meter-long baseline in an attempt to estimate the range precision of a Cyrax 2400 3D laser scanner. Least squares estimation

was used to fit the planes to each target scan cloud. An analysis of the point deviation from this plane produced point residuals, which in turn produced an overall RMS statistic for each target plane. Based on root mean square (RMS) measurements, the range error was inspected to be between 3 and 15 mm in the 20 m pillars. Later, Lichti et al. revealed similar findings in [15] and [16] following EDM calibration baseline tests. The authors revealed the impact of laser device eccentricity on the range-uncertainty level in close-ranging measurements. Kersten et al. [17] applied a similar range-evaluation routine to a 100 m baseline range to a TLS device. Plane and sphere targets were used to validate the measurements based on spherical adaptors. They analyzed the results with reference measurements and found discrepancies that reached up to 3.4 mm further from the reference distance to the plane targets. However, the distances were reported to reach 8.3 mm further than the reference distances in the cases of the spheres. This indicated that sphere point clouds produced more dispersion than plane point clouds, which is considered to be a major problem in range measurements. Furthermore, larger errors (>100 mm) were reported by [18] by using a similar approach.

As for the Stonex X300 TLS device, limited studies reported the potential of close-range measurements that were obtained from this device in different applications. The Stonex X300 is still considered to be a new TOF device from the Stonex positioning company [19]. Similar to most TOF scanners, The Stonex X300 was found to be more relevant for mid-range measurements than it was in close-range measurements due to its measuring principals (which are based on the pulse-ranging technique – as with most similar scanner devices) [4, 20]. Even though this laser device is featured in limited range-analysis studies [21], the available studies have revealed the sufficiency of this device for close-range measurements if the measurements have analyzed and signal-to-noise error impacts that are correctly eliminated. For example, [22] presented a practical study to use the Stonex X300 for structural health monitoring (SHM) in a close-range environment. The authors presented their initial insights to measure cracks in building structures using this device. The outcomes showed precise measurements and delivered valuable results that reached sub-centimeter levels.

Later, [23] used the Stonex X300 to document the famous Lamassu heritage monument (located in Iraq) from the ancient Mesopotamian civilization era. The authors revealed that they could successfully remove the unreliable measurements from close-range observations following accurate 3D data filtering (including scan-incidence angle masking and noise-outlier filtering). The minimum scan range of this device was found to be 2.5 m following their practical indoor and outdoor experiments [23]. Under perfect conditions, less than 4 mm was the range accuracy that was delivered for the Lamassu statue in this study. This outcome revealed the importance of range measurement analysis for reducing erroneous noise, roughness, and incident-angle effects before the registration process. Similar conclusions were drawn by [20], who studied the ranging precision of Stonex X300 measurements

following a user-design scheme. In this study, the influence of the range-measure variations was analyzed using fixed device setting for ranges between 5 and 200 m. The authors delivered an approximate steady variation within a range precision of 5 to 150 m; however, the differences started to increase rapidly past the 75 m range in outdoor environments. They also analyzed the range precision under different weather conditions.

Consequently, [24] presented a study toward overcoming the limitations of individual techniques by fusing range-based and image-based measurements using the Stonex X300 device. The authors delivered laser data in close ranging and used structure from motion multi-view stereo (SfM-MVS) photogrammetry in order to optimize cultural heritage conservation methodologies. The study presented a comparison between the laser-scanning potential and photogrammetry in terms of range accuracy, scanning time, data density, level of automation, budgeting, and affordability. For high LOD requirements, laser-data roughness was considered to be a challenge in this study. They claimed high levels of roughness in the Stonex X300 measurements, which were possibly acquired due to the range finder's accuracy and/or the device's internal signal-processing algorithms. Later, [25] proposed a developed data-fusion routine with photogrammetry to improve the Stonex X300's measurement productivity for 3D modeling applications. In this study, reducing the levels of noise in the close-range measurements was a priority (especially in the authors' indoor experiments). Therefore, they applied careful application settings of the filtering masks and proved the effectiveness of the Stonex X300's close-range measurements by successfully reducing the incidence-angle effects of the scanner laser beams.

As the Stonex X300 is more affordable than many other expensive TOF scanners for limited-budget projects, there is a necessity to analyze the positional behavior of its measurements against range changes. This is important for highlighting the limitations of its close-range measurements according to a fixed range increment. Therefore, the main goal of our research is to analyze the behavior of the device measurements and present a technical workflow in order to limit the uncertainty levels in close-range measurements.

2.   Method

The methodology that is presented in this research is based on range-uncertainty analysis and validation checking according to reference measurements in an indoor environment. The methodology analyzes the positional accuracy results that were delivered from the range-based technique with those that were obtained from the image-based technique using similar conditions to show the potential in close ranging. Figure 1 highlights the main method steps in the implemented workflow.
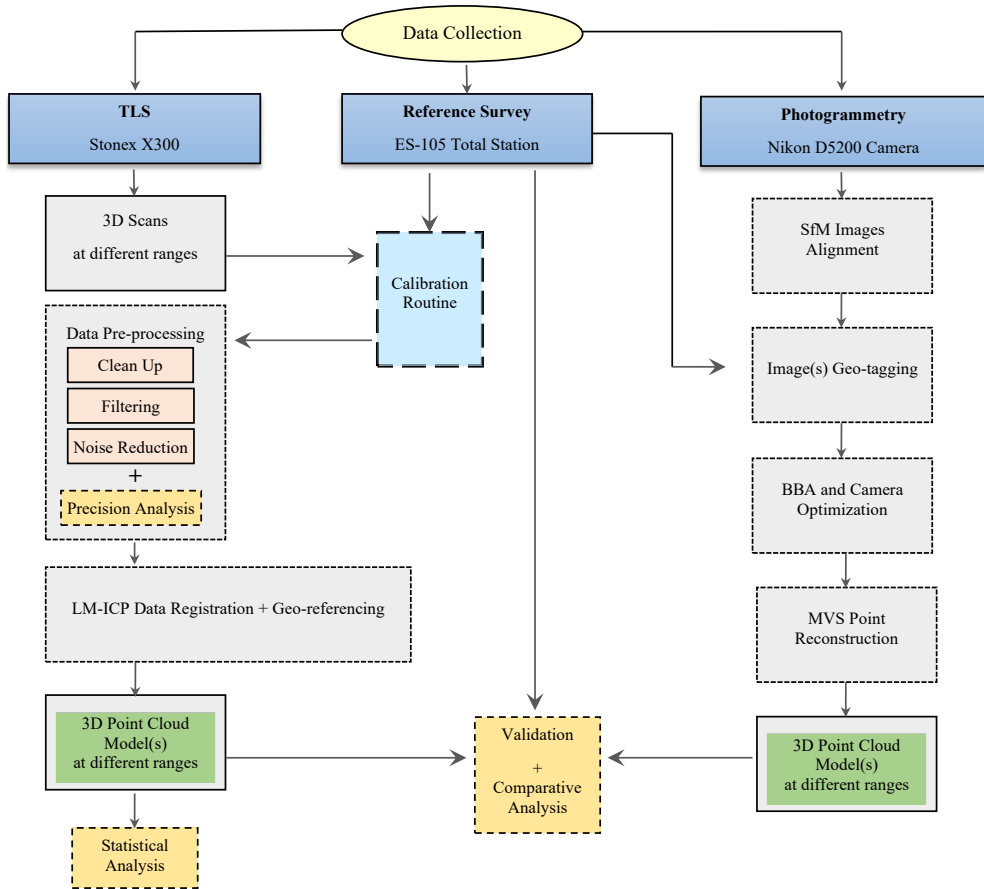
Fig. 1. Diagram of methodology workflow

2.1. Range-based Uncertainty Measure

The method aims to study the impact of range variation on the positional behavior of the Stonex X300's close-range measurements. The technical specifications of this device are listed in Table 1. One of the main errors that affect laser measurement is the level of noise that is inherent within the sensor [12, 25], which can be highly noticed in the Stonex X300's close-range measurements [26]. This is mainly acquired as a result of laser-beam-propagation errors, the mixed-edge problems that are obtained from a scanned object, range and angular uncertainty, and axis-misalignment errors [1, 27, 28]. The laser-beam-propagation errors come from the effects that are obtained from widening a laser beam along the travel distance that increases as the distance increases between the laser transmitter and the scanned object [29, 30]. This beam-widening is called laser beam divergence [4]. The divergence of the laser beam

can highly affect the positional uncertainty of a laser measure; this can be expressed as follows [1]:

$$w(p_w) = w_0 \cdot \sqrt{1 + \left(\frac{\lambda \cdot p_w}{\pi \cdot w_0^2} \right)^2} \tag{4}$$

where p_w is the range value according to the beam waist location, w is the radius of the laser beam, w_0 is the beam waist at the transmitting point (which represents the minimum beam radius), and λ is the wavelength of the beam.

Table 1. Technical parameters of Stonex X300 3D laser scanner

Parameter	Setting
Range	1.6–300 m
Scan rate	up to 40,000 pt./s
Field of view (FOV)	horizontal: 360° vertical: 90° (−25° to +65°)
Laser beam diverge	0.076° × 0.029°
Laser angular resolution	horizontal: 1.35′ vertical: 1.35′
Density	39 mm × 39 mm at 100 m
Range accuracy	<6 mm at 50 m <40 mm at 300 m
Laser wavelength	905 nm (invisible)
Integrated camera resolution	192 megapixel (MP) over 360°

Source: http://www.stonex.it

On the other hand, the positional accuracy of the laser beam is highly affected by range measure uncertainty that is computed according to the laser-measuring system. The range uncertainty can be expressed as a function of multiple parameters based on the sensor type and its working principals and measuring mechanism (as follows) [4]:

$$\delta_z \approx \frac{C \cdot T_t}{2 \cdot \sqrt{SNR}} \tag{5}$$

where δ_z is the range uncertainty, C is the speed of light, T_t is the laser pulse rise time (this usually depends on the clocking mechanism), and SNR is the signal-to-noise ratio. This model represents the range uncertainty that is inherent to all TOF scanner systems [13].

Following this, an empirical approach was applied in this research in order to detect the precision of the Stonex X300's measurements. An old EDM device was selected as the area of interest (AOI). The upper part of the device was covered with a cardboard box to facilitate the stacking of the coded targets and deliver an extended surface (see Fig. 2). This object was selected to keep the impact of the level of complexity to a minimum as much as possible. It was planned to investigate the impact of the range dependency within a 30 m range and make measurements at every 5 m range interval. Due to space limitations, the selected object was mounted on a turntable to help rotate the scanned object during the data-capturing process while setting the scanner device at the selected ranges.
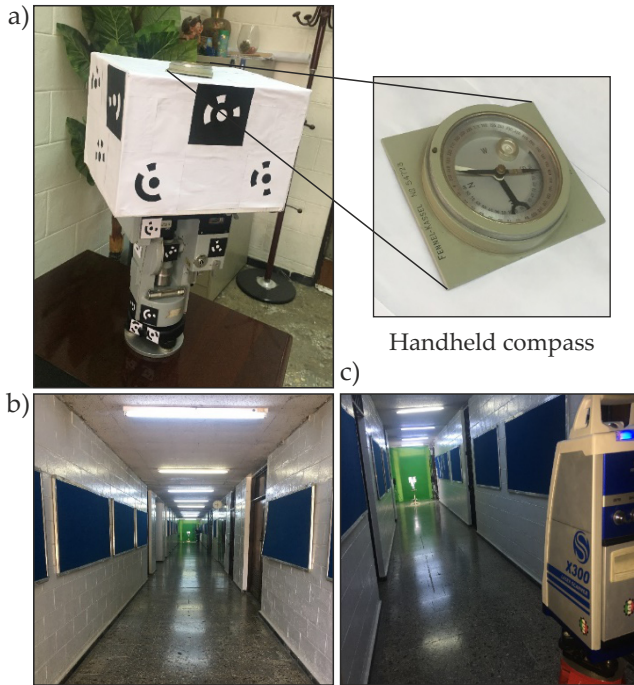

Handheld compass

Fig. 2. Range analysis experiment:
a) object of interest; b) indoor scan environment; c) laser data collection process

A counter-clockwise rotation was applied with a fixed angle increment (30°) of a 360° total range rotation. This was set in order to cover the entire scanned object from all sides; to guarantee the fixed-angle-increment orientation, a compass was installed above the cardboard box. The scanning process was applied in multiple scans for individual stations between 5 and 30 m. The scan was performed every 30° to maintain a convenient overlap percentage between successive scans. Following this setup, 12 scans were delivered at every station with a 5 m range increment from 5

to 30 m ranges. These overlapped scans were later pre-processed and filtered using native JRC 3D Reconstructor software (www.gexcel.it) in order to exclude any outliers that could have reduced the registration outcomes [31]. The software can provide multiple filtering tools in this respect, such as noise reduction based on normal vector computation, incident-angle thresholding, and masking points based on the AOI type and material [26].

A registration process was applied to link the scans that were obtained from successive scan stations and collected at different rotation angles in one AOI local-coordinate system. To deliver a high level of accuracy, the registration process was implemented by using the available coded targets that were detected automatically (see Fig. 3). The registration process is a crucial step in laser-data processing, as the relative geometric quality of the data is mainly based on this step [8, 9]. Therefore, selecting the optimal registration strategy and adequate setting parameters is highly important for optimal accuracy standards [30]. First, the points are roughly registered based on manual registration to facilitate the automatic target-detection and registration process. However, the automatic registration was implemented using the rotation angle that was obtained from the manual process as an input to the iterative closest registration (ICP) process. Finally, the global-wise automatic-registration approach was applied using the Levenberg–Marquardt iterative closest points (LM-ICP) algorithm to refine the results and reduce the global registration error [4, 23]. The LM-ICP registration was based on the least squares (LS) adjustment bundle to decrease the discrepancies among the scans in the X, Y, and Z directions in one single solution. This helped to evenly distribute any errors among the scans toward optimal adjusted values [8, 32]. Following a successful automatic workflow, the registration errors between overlapping scans were successfully reduced to approximately 2 mm in the 5 m range and to 5.8 mm in the 30 m range.
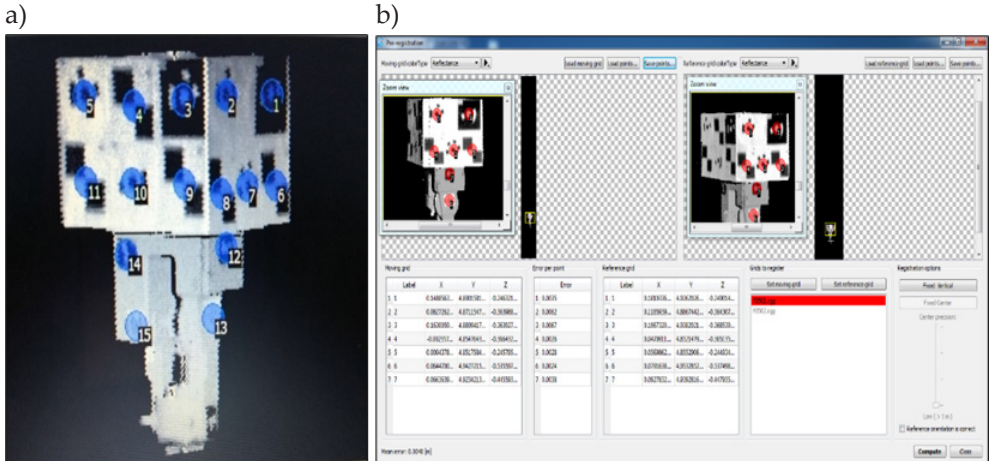
a)   b)

Fig. 3. Pre-ICP registration showing coded-target tagging (a) and LS application (b)

The 3D point clouds were georeferenced based on the ground truth measurements and later adjusted for validation purposes. It is worth mentioning that the geo-referencing process was applied based on the error-free assumption of the reference target measurements that were obtained from the ES-105 total station device. Furthermore, the empirical approach that was implemented in this research was based on calibrating the Stonex X300 device following the user-oriented routine that was explained in [21].

2.2. Image-based Uncertainty Measure

In this study, the coded targets were designed to meet the accuracy requirements in both the range-based and image-based techniques. This was intended for a later comparison with the photogrammetric approach following the application of the structure from motion multi-view-stereo (SfM-MVS) algorithms of the data that was obtained under the same conditions and experimental design. However, as the illumination in the photogrammetric approach is a vital parameter (which is not necessarily the case in laser scanning), the lighting conditions of the AOI were considerably improved by using an external light source. It is generally desired to keep the camera's ISO value as minimal as possible, thus reducing the levels of noise in the collected images. For this purpose, a Nikon D5200 camera (6000 × 4000 pixels) with a 24.10 megapixel resolution was used to deliver the images with a nearly 85% forward overlap (see Fig. 4).
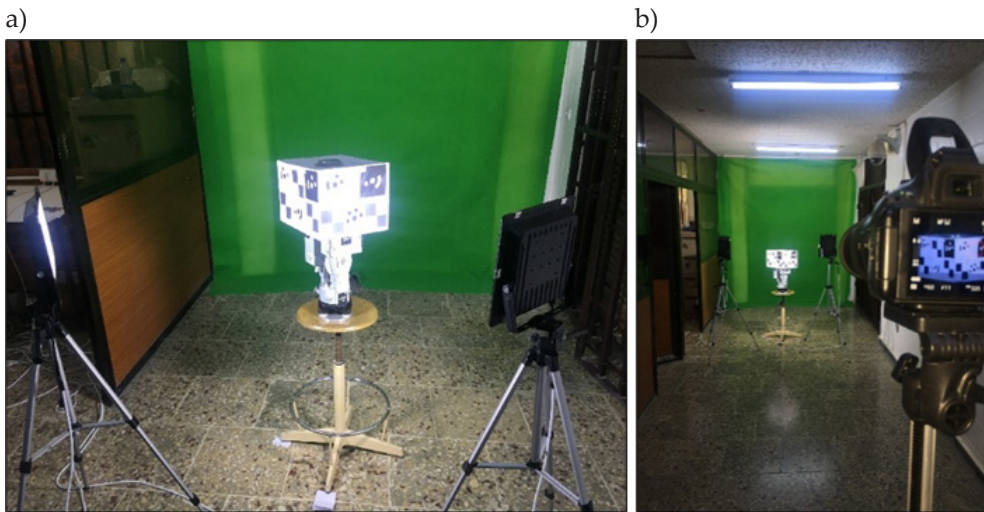
a)   b)

Fig. 4. Photogrammetric data-collection session
showing light conditions (a) and camera settings (b)

The image-acquisition plan was set to capture three overlapping images from each station in the vertical direction, with a nearly 60% side overlap to increase the

redundancy ($K = 3$) (Equations (6)–(8)). The camera position was selected at the same reference points that were used to set the laser scanner in the range-based approach. This plan setting was able to increase the estimated accuracy of the extracted 3D data by detecting matched pairs and delivering accurate camera trajectory positions [33]:

$$\sigma_{XYZ} = \frac{q \cdot S \cdot \sigma_{XY}}{\sqrt{k}} \tag{6}$$

$$S = \frac{f}{H} \tag{7}$$

$$H = \frac{f \cdot GSD}{PS} \tag{8}$$

where σ_{XYZ} represents the estimated error in the computed object coordinates, q is the design factor that refers to the strength of the camera capture plan, S is the scale factor that is defined by the camera's focal length (f) and the depth distance (H) between the camera and the ground target, and σ_{XY} refers to the estimated error in the photo coordinates. GSD refers to the ground sample distance that the user intends to approach, while PS refers to the image pixel size; the latter can be computed as follows:

$$PS = \frac{CX}{PX} \tag{9}$$

where CX represents the camera sensor size, and PX refers to the number of pixels. The sensor size is based on the camera type and the factory specifications; however, the number of pixels is based on the image frames of the camera (see Table 2).

Table 2. Camera parameters in photogrammetric data-collection session

Parameter	Setting
Resolution	24.10 megapixel (MP)
Sensor size	23.5 mm ×15.6 mm (APS-C)
Focal length	300 mm (external lens)
Overlap	end lap: 85% side lap: 60%
Image size	6000 × 4000 pixels (large frame)
Camera ISO	200
Aperture value	f13
Shutter speed	0.6 s
Depth distance	5–30 m

The photo-alignment process following the SfM algorithms was applied using Agisoft Metashape software (www.agisoft.com). The turntable was rotated after each image-capture set following the same acquisition strategy that was explained earlier in the laser measurements. In the individual image set, the horizontal movement was set at every 30° in order to deliver an 85% overlap percentage between the images in the horizontal direction. In the vertical direction, however, the camera has set to collect three images of different orientations at each station in order to deliver a 60% side-lap coverage.

3. Results and Discussion

3.1. Precision Analysis

As previously stated, all TOF scanners deliver a certain level of noise (roughness) from close-range measurements. This scanning delivers noisy data from short-range acquisition scans due to the various incident angles of the transmitted signals and the SNR of the range-finder system. Therefore, it was necessary to adopt a noise-reduction routine before applying any error analysis of the individual scans. In this respect, the scans were carefully filtered to reduce the noise amounts and eliminate any outlier measurements. This process needs to be applied with care by selecting the optimal parameters in order to clean the data from the weak return signals that are delivered from the edge areas and critical incidence angle values.

The roughness level could be estimated based on the Euclidian distance that was computed between the individual points and the best-fitting plane. In this case, the kernel size was based on the radius of the selected sphere and was centered at the individual points [34]. The distances were computed from the nearest neighbor points based on octree computations [6, 11]. Following this, the level of noise was successfully reduced (see Figure 5, which shows the results at a 5 m range).
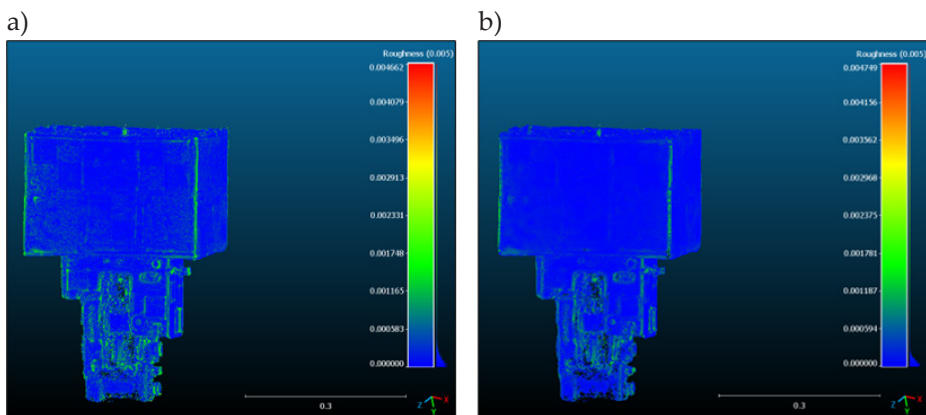
a)   b)

Fig. 5. Roughness analysis at 5 m range: a) before noise reduction; b) after noise reduction

However, the reduction in the mean error was gradually decreased as the range increased to 30 m. The results proved the validity when the data was correctly analyzed and the error uncertainty was manipulated correctly to reduce the noise level. This was based on the careful selection of the kernel parameter that was used in the roughness tool and the roughness-assumption algorithm [35]. It is worth mentioning that the level of noise in the Stonex X300's range measurements increased as the range decreased and approached the minimum range of the range-finder component (see [23] for further details).

3.2. Accuracy Analysis

Thirty coded targets were used to assess the accuracy of the Stonex X300's measurements in this study. These targets were mounted on the AOI and used for the quality-assessment analysis. This analysis included measurements that were delivered from six different ranges (5, 10, 15, 20, 25, and 30 m). These targets were divided into 20 laser-coded targets plus 10 extra photogrammetric targets (refer to Figure 2). The accuracy analysis aimed to investigate the behaviors of the individual laser measurements in the 3D-coordinate directions as a function of range between 5 and 30 m (at 5 m intervals). The data was collected from the overlapped scans at the individual scan stations by turning the turntable counterclockwise in 30° increments. The workflow delivered 12 overlapping scans from the individual scan stations between 0° and 360°. The scans were processed (including filtering and LM-ICP registration) and later exported for a statistical analysis.

Figure 6 (on the interleaf) demonstrates the fitting analysis of the 30 coded target measurements based on the WGS84 reference coordinate system in the 3D axis. The simulation showed the positional behavior of these measurements as the range increased at the fixed increments. It can be noticed that a nearly perfect match was delivered in the X direction at a 5 m range, while the deviations increased as the range increased in the same direction. Nearly similar behavior was reported in the Y direction; however, some outlier measurements could be noticed. These errors might have been acquired due to erroneous target center computations in the registration process.

In contrast, the results that were delivered from the Z direction showed nearly steady positional behaviors in all of the measurements (with a few variations noticed in multiple points). These findings are also revealed in Figure 7 (on the interleaf) when all of the range measurements are combined to fit in a single plot for the individual X, Y, and Z directions. This behavior proved that vertical laser measurements could deliver a stable accuracy level from close-range measurements – even when the scan range increased. The horizontal accuracy was still better than the vertical accuracy in those ranges that were close to the minimum (e.g., 5 and 10 m). This may have been acquired due to the careful noise-reduction process that was applied before the data registration. However, the overall results were still in line and matched the range-accuracy findings of the other TOF scanners [7, 13, 16, 20]. This was only valid as long as the device was set to measure distances within the manufacturer's range-limitation settings.
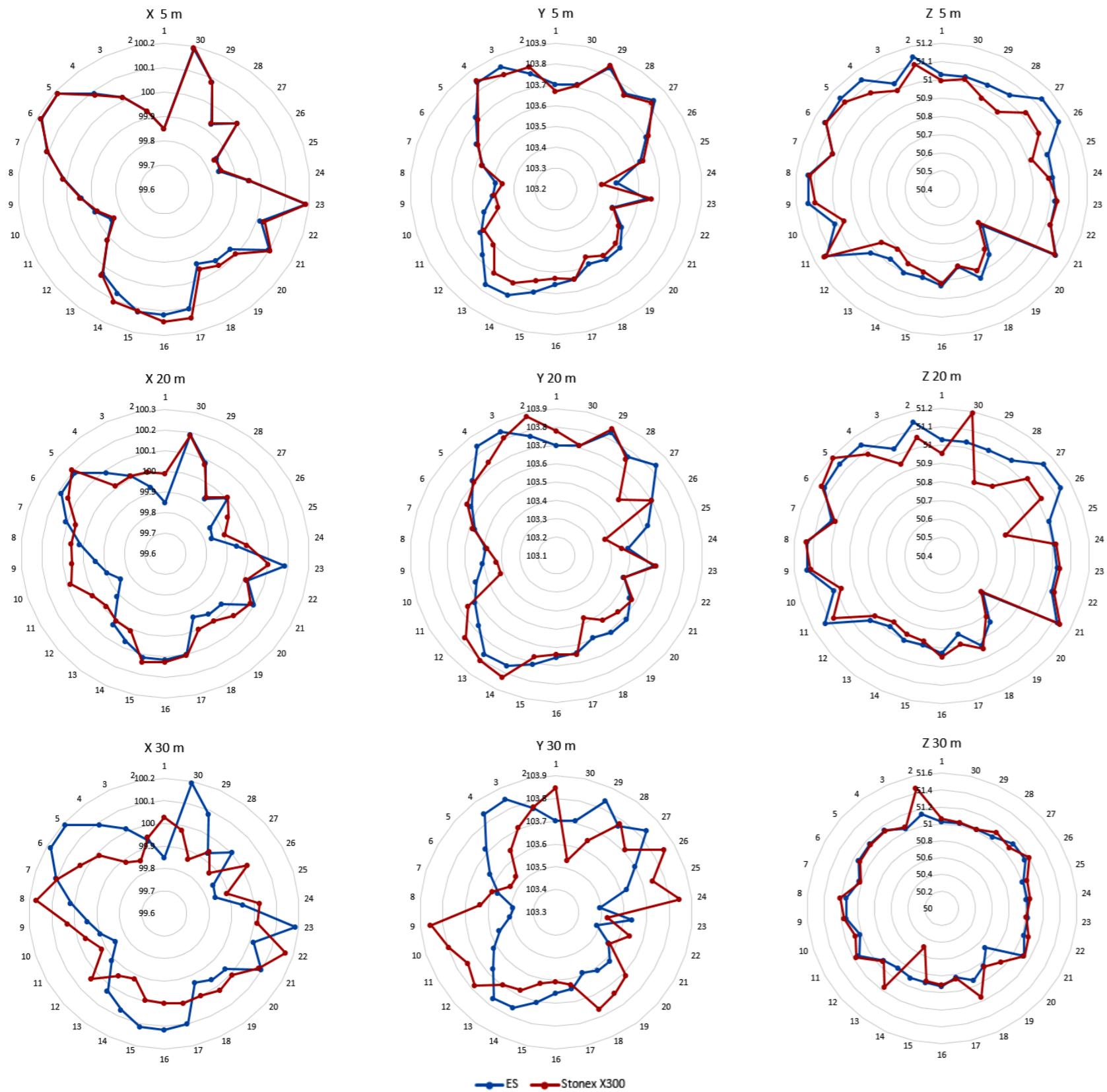
Fig. 6. Fitting Stonex X300 point-difference measurements to reference ES device measurements of 30 targets at 5, 20, and 30 m ranges in X, Y, and Z directions
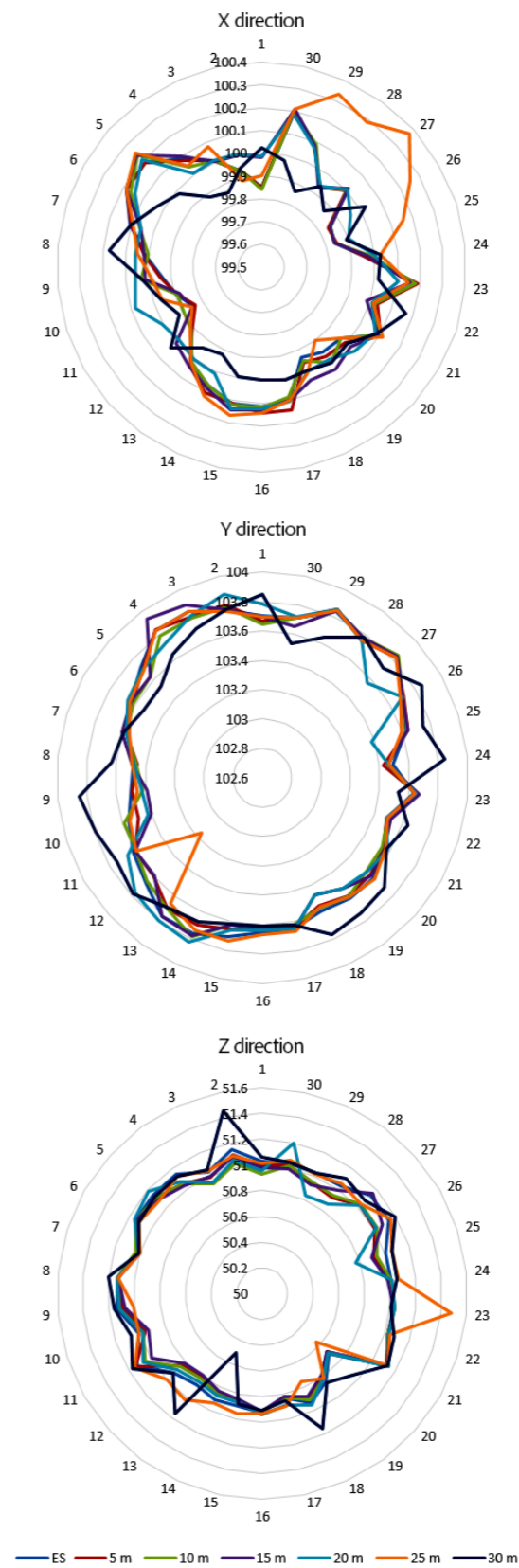

Fig. 7. Combined fitting results of Stonex X300 point differences to reference ES device measurements of 30 targets at 5 to 30 m ranges in X, Y, and Z directions

Consequently, we could clearly observe the fitting variations with the reference values between the horizontal and vertical directions when comparing the minimum and maximum range-measurement results. This simulation is demonstrated in Figure 8 for the 5 and 30 m ranges only. This figure shows a few variations in the vertical direction in contrast with the higher variations that were obtained in the horizontal direction. However, the results still showed a higher accuracy level at the 5 m range when compared to those that were obtained at the 30 m range in both directions.
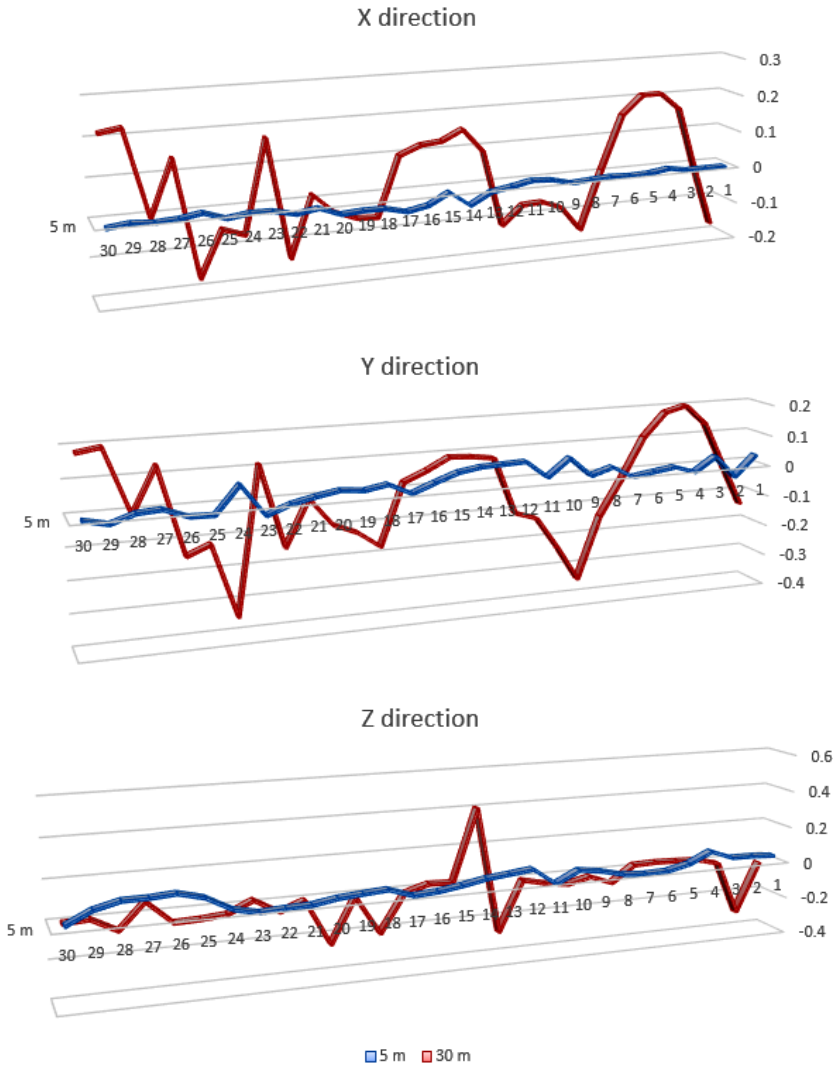

Fig. 8. Stonex X300 point-difference measurements of 30 targets
at 5 m and 30 m ranges – showing variations in X, Y, and Z directions

To simulate these findings, the differences between the laser and reference measurements were computed; these were simulated by using box plots in the individual 3D directions (see Fig. 9). These results showed the distinct rise in the error differences that were obtained in the horizontal direction as the range increased; this was in contrast with the behavior of the positional accuracy in the vertical direction.
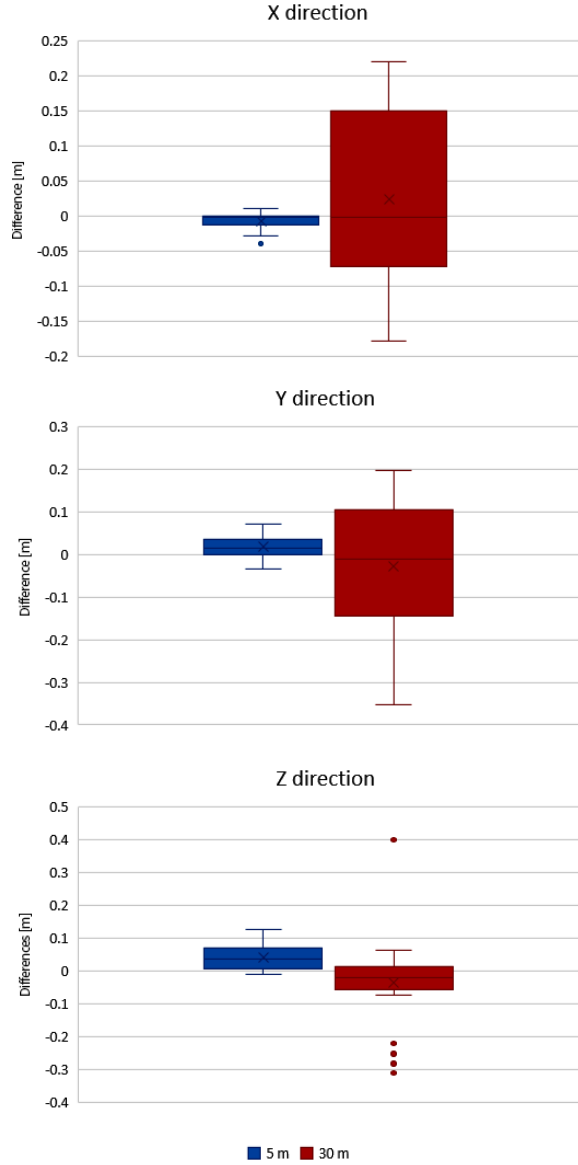

Fig. 9. Box plots of Stonex X300 difference measurements
at 5 m and 30 m ranges in X, Y, and Z directions

3.3. Validation and Comparative Analysis

A validation analysis was applied to check the absolute accuracy of the Stonex X300 target measurements that were obtained at the 5, 10, 15, 20, 25, and 30 m ranges based on the referenced ground-truth measurements. The root mean square error (RMSE) values were computed and analyzed from the individual measurements in order to check the validity (see Fig. 10). It can clearly be seen that the laser measurements delivered better accuracy in the horizontal direction than they did in the vertical direction; however, these errors remained within a one-centimeter level in both directions. These errors increased as the ranges increased in all directions, and no outliers were highlighted.

To provide a comparative analysis between the range-based and image-based techniques, a simulation analysis was also applied using the measurements being delivered from photogrammetry following the data-acquisition plan that was explained in Section 2.1. The RMSEs were computed and analyzed based on the same coded-targets (see Fig. 11).
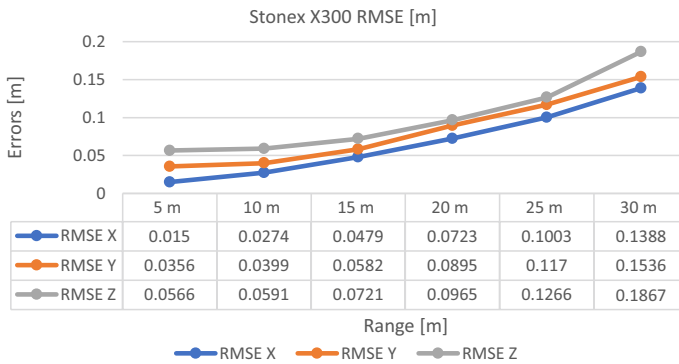
Stonex X300 RMSE [m]

	5 m	10 m	15 m	20 m	25 m	30 m
RMSE X	0.015	0.0274	0.0479	0.0723	0.1003	0.1388
RMSE Y	0.0356	0.0399	0.0582	0.0895	0.117	0.1536
RMSE Z	0.0566	0.0591	0.0721	0.0965	0.1266	0.1867

Fig. 10. Validation analysis of laser-range measurements in X, Y, and Z directions

Photogrammetry RMSE [m]

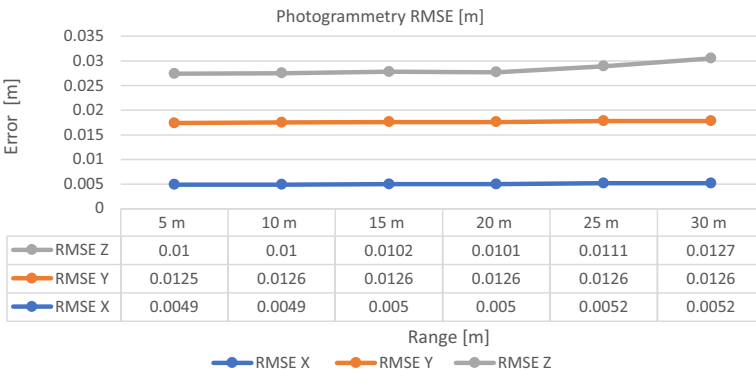|	5 m	10 m	15 m	20 m	25 m	30 m
RMSE Z	0.01	0.01	0.0102	0.0101	0.0111	0.0127
RMSE Y	0.0125	0.0126	0.0126	0.0126	0.0126	0.0126
RMSE X	0.0049	0.0049	0.005	0.005	0.0052	0.0052

Fig. 11. Validation analysis of photogrammetric measurements in X, Y, and Z directions

It can be noticed that the accuracy that was obtained from photogrammetry remained nearly the same in all directions whenever the range increased (which was in contrast with the laser results). A slight increase in the errors could be noticed when the range increased; however, the accuracy level was still steady within the 30 m tested range, and no dramatic change was highlighted.

When compared to the Stonex X300 results, the photogrammetry outcomes showed superiority in spite of of the limited accuracy level that was obtained in this experiment due to the low illumination conditions. This proved the effect of the AOI illumination conditions, which negatively deteriorated the result outcomes from photogrammetry. Therefore, it is recommended to apply the same experiment in an outdoor environment to show the effect of the illumination conditions on the accuracy outcomes, as this can highly affect the laser intensity and image quality. However, these outcomes were obtained for the range limits that were specified in this study and should not be generalized for all close-range measurements.

Following these outcomes, photogrammetry proved to obtain a better accuracy performance than the Stonex X300's laser measurements in both the horizontal and vertical directions in close-ranging. This may be justified, as range-based measurements are influenced by many error sources, such as laser range-finder accuracy, the threshold of laser-echo detection, surface-interaction conditions, etc. [10].

The range-based measurements were also affected by the target material, the filtering and registration shortcomings, and the data smoothness; these could have highly affected the correct estimation of the target center. This was not the case for photogrammetry, as point detection in image-based techniques is much easier than that of laser scanning. However, photogrammetry is highly impacted by the image resolution and pixel size as related to the sensor type and camera settings.

Although the photogrammetric measurements obtained a much more regular error pattern than the Stonex X300 laser measurements, the horizontal accuracy in photogrammetry was still better than the vertical accuracy. This can be easily noticed from the RMSE values that are highlighted in Figure 11. In contrast, the laser-accuracy-validation results showed a regular increment in their accuracy levels as the range increased (in spite of the slight drawback that was obtained in the X and Y directions at the 25 and 30 m ranges, respectively). This could potentially highlight the impact of the careful noise-reduction routine that was applied earlier to the registration process. However, these results need to be further investigated with greater ranges for the better possible error modeling of the Stonex X300's measurements.

4. Conclusions

This research presents a new study of error-analysis and range-uncertainty performance of laser measurements that were obtained from the brand-new Stonex X300 TLS device. The methodology was based on an empirical approach for

analyzing measurements in an indoor environment and investigating the impact of range dependency on the geometric positioning behavior up to a 30 m range. The outcomes that were obtained from this research reported that the Stonex X300's measurements behaved in a similar fashion to other TOF scanners; however, more care should be taken with very close ranges. The delivered measurements corresponded with general laser device performance, where the accuracy decreases whenever the range increases. However, the accuracy results showed a significant improvement following the careful selection of the noise settings. This included cleaning the data from the weak return signals that were obtained from the high-incidence angle measurements (especially in the edge areas). This seemed to improve the critical signal thresholds that were applied by the laser range-finder unit. The careful selection of the noise-filtering parameters affected the accuracy of the outcomes that were delivered from this device in both the horizontal and vertical directions. It could also be found that the Stonex X300 delivered more-stable measurements in the vertical direction as compared to the horizontal direction – even when the range increased. However, the precision level in the vertical direction was better than that of the horizontal direction. Future studies will include focusing on error modeling in larger ranges in both indoor and outdoor environments as well as independently investigating the effects of angular errors in the Stonex X300's measurements.

Author Contributions

Fanar M. Abed: proposal and research conceptualisation; planning and structuring; data acquisition; formal analysis; investigation; methodology; data validation; writing and editing.

Luma K. Jasim: data acquisition; formal analysis; writing.

Marwa M. Bori: data acquisition; formal analysis.

All of the authors have read and agreed to the published version of the manuscript.

References

[1] Santana Quintero M., Van Genechten B., De Bruyne M., Poelman R., Hankar M., Barnes S., Caner H., Budei L., Heine E., Reiner H., Lerma García J.L., Biosca Taronger J.M.: *Theory and Practice on Terrestrial Laser Scanning: Training Material Based on Practical Applications*. Universidad Politecnica de Valencia Editorial, Valencia, 2008.

[2] Karkush M., Choudhury D., Han J. (eds.): *Current Trends in Geotechnical Engineering and Construction: Proceedings of 3ICGE-Iraq 2022*. Springer, Singapore 2022. https://doi.org/10.1007/978-981-19-7358-1.

[3] Vosselman G., Maas H.-G. (eds.): *Airborne and Terrestrial Laser Scanning*. Whittles Publishing, Dunbeath 2010.

[4] Shan J., Toth Ch.K. (eds.): *Topographic Laser Ranging and Scanning: Principals and Processing*. 2nd ed. CRC Press, Boca Raton 2017. https://doi.org/10.1201/9781315154381.

[5] Manferdini A.M., Remondino F.: *A review of reality-based 3D model generation, segmentation and web-based visualization*. International Journal of Heritage in the Digital Era, vol. 1(1), 2012, pp. 103–123. https://doi.org/10.1260/2047-4970.1.1.103.

[6] Abed F.M., Mills J.P., Miller P.E.: *Calibrated full-waveform airborne laser scanning for 3D object segmentation*. Remote Sensing, vol. 6(5), 2014, pp. 4109–4132. https://doi.org/10.3390/rs6054109.

[7] Medić T., Kuhlmann H., Holst C.: *Empirical evaluation of terrestrial laser scanner calibration strategies: Manufacturer-based, target-based and keypoint-based*. [in:] Kopáčik A., Kyrinovič P., Erdélyi J., Paar R., Marendić A. (eds.), *Contributions to International Conferences on Engineering Surveying: 8th INGEO International Conference on Engineering Surveying and 4th SIG Symposium on Engineering Geodesy*, Springer Proceedings in Earth and Environmental Sciences, Springer, Cham 2021, pp. 41–56. https://doi.org/10.1007/978-3-030-51953-7_4.

[8] Cheng L., Chen S., Liu X., Xu H., Wu Y., Li M., Chen Y.: *Registration of laser scanning point clouds: A review*. Sensors, vol. 18(5), 2018, 1641. https://doi.org/10.3390/s18051641.

[9] Schmitz B., Holst C., Medic T., Lichti D.D., Kuhlmann H.: *How to efficiently determine the range precision of 3D terrestrial laser scanners*. Sensors, vol. 19(6), 2019, 1466. https://doi.org/10.3390/s19061466.

[10] Muralikrishnan B.: *Performance evaluation of terrestrial laser scanners – A review*. Measurement Science and Technology, vol. 32(7), 2021, 072001. https://doi.org/10.1088/1361-6501/abdae3.

[11] Fowler A., Kadatskiy V.: *Accuracy and error assessment of terrestrial, mobile, and airborne lidar*. [in:] *American Society for Photogrammetry and Remote Sensing Annual Conference 2011, Milwaukee, Wisconsin, USA, 1–5 May 2011*, American Society for Photogrammetry and Remote Sensing (ASPRS), 2011, pp. 135–143. http://www.asprs.org/a/publications/proceedings/Milwaukee2011/files/Fowler_1.pdf.

[12] Alkan R.M., Karsidag G.: *Analysis of the accuracy of terrestrial laser scanning measurements*. [in:] *FIG Working Week 2012: Knowing to manage the territory, protect the environment, evaluate the cultural heritage, Rome, Italy, 6–10 May 2012*, pp. 1–16. https://www.fig.net/resources/proceedings/fig_proceedings/fig2012/papers/ts07a/TS07A_alkan_6097.pdf.

[13] Shi S., Muralikrishnan B., Sawyer D.: *Terrestrial laser scanner calibration and performance evaluation using the network method*. Optics and Lasers in Engineering, vol. 134, 2020, 106298. https://doi.org/10.1016/j.optlaseng.2020.106298.

[14] Gordon S., Lichti D.D., Stewart M.P., Tsakiri M.: *Metric performance of a high-resolution laser scanner*. [in:] El-Hakim S.F., Gruen A. (eds.), *Videometrics and Optical Methods for 3D Shape Measurement*, SPIE Proceedings, vol. 4309, SPIE, 2000, pp. 174–184. https://doi.org/10.1117/12.410872.

[15] Lichti D.D., Stewart M.P., Tsakiri M.: *Benchmark tests on a three-dimensional laser scanning system.* Geomatics Research Australasia, vol. 72, 2000, pp. 1–23.

[16] Lichti D.D., Stewart M.P., Tsakiri M., Snow A.J.: *Calibration and testing of a terrestrial laser scanner*. The International Archives of the Photogrammetry, Remote Sensing and Spatial Information Sciences, vol. XXXIII-B5, 2000, pp. 485–492. https://www.isprs.org/proceedings/XXXIII/congress/part5/485_XXXIII-part5.pdf.

[17] Kersten Th., Sternberg H., Mechelke K., Pardo Acevedo C.: *Terrestrial laserscanning system Mensi GS100 – Accuracy tests, experiences and projects at the Hamburg University of Applied Sciences*. The International Archives of the Photogrammetry, Remote Sensing and Spatial Information Sciences, vol. XXXIV-5/W16, 2004, pp. 1–8. https://www.isprs.org/proceedings/XXXIV/5-W16/papers/PanoWS_Dresden2004_Kersten.pdf.

[18] Zhang Y., Wu H., Cheng X., Liu C.: *Accuracy evaluation of three dimensional laser range scanner based on field calibration*. [in:] Li D., Ge Y., Foody G.M. (eds.), *Accuracy in Geomatics: Proceedings of the 8th International Symposium on Spatial Accuracy Assessment in Natural Resources and Environmental Sciences: Shanghai, China, June 25–27, 2008. Volume 2*, World Academic Union (World Academic Press), Liverpool 2008, pp. 119–126.

[19] Stonex X300. https://www.stonex.it/ [access: 5.10.2020].

[20] Ding H., Lin H., Wang X.: *Ranging precision analysis of Stonex X300 3D laser scannerd*. IOP Conference Series: Materials Science and Engineering, vol. 423, 2018, 012146. https://doi.org/10.1088/1757-899X/423/1/012146.

[21] Abed F.M., Jasim L.K., Bori M.M.: *User oriented calibration method for Stonex X300 terrestrial laser scanner*. Iraqi Journal of Science, vol. 64(4), 2023, pp. 2095–2106. https://doi.org/10.24996/ijs.2023.64.4.43.

[22] Abed F.M., Ibrahim O.A., Jasim L.K., Hussein Z.E.: *Terrestrial laser scanning to preserve cultural heritage in Iraq using monitoring techniques* [conference paper]. BCEE 2015: The Second International Conference on Buildings, Construction and Environmental Engineering, October 17–October 18, 2015, Beirut, Lebanon. https://doi.org/10.13140/RG.2.1.1306.1600.

[23] Shanoer M.M., Abed F.M.: *Evaluate 3D laser point clouds registration for cultural heritage documentation*. The Egyptian Journal of Remote Sensing and Space Sciences, vol. 21(3), 2018, pp. 295–304. https://doi.org/10.1016/j.ejrs.2017.11.007.

[24] Jaber A.S., Abed F.M.: *Revealing the potentials of 3D modelling techniques; a comparison study towards data fusion from hybrid sensors*. IOP Conference Series: Materials Science and Engineering, vol. 737, 2020, 012230. https://doi.org/10.1088/1757-899X/737/1/012230.

[25] Jaber A.S: *The Fusion of Laser Scans and Digital Images for Effective Cultural Heritage Conservation* [MSc thesis]. Department of Surveying Engineering, College of Engineering, University of Baghdad, 2020. https://doi.org/10.13140/RG.2.2.29736.39683.

[26] Thamir Z.S., Abed F.M.: *How geometric reverse engineering techniques can conserve our heritage; a case study in Iraq using 3D laser scanning*. IOP Conference Series: Materials Science and Engineering, vol. 737, 2020, 012231. https://doi.org/10.1088/1757-899X/737/1/012231.

[27] Abed F.M., Mills J.P., Miller P.E.: *Calibration of full-waveform ALS data based on robust incidence angle estimation*. The International Archives of the Photogrammetry, Remote Sensing and Spatial Information Sciences, vol. XXXVIII-5/W12, 2011, pp. 25–30. https://doi.org/10.5194/isprsarchives-XXXVIII-5-W12-25-2011.

[28] Kadhim I., Abed F.M., Vilbig J.M., Sagan V., DeSilvey C.: *Combining remote sensing approaches for detecting marks of archaeological and demolished constructions in Cahokia' s Grand Plaza, Southwestern Illinois*. Remote Sensing, vol. 15(4), 2023, 1057. https://doi.org/10.3390/rs15041057.

[29] Holst C., Neuner H., Wieser A., Wunderlich T., Kuhlmann H.: *Calibration of terrestrial laser scanners*. Allgemeine Vermessungs-Nachrichten (AVN), vol. 123(6), 2016, pp. 147–157. https://hdl.handle.net/20.500.11811/8764.

[30] Kadhim I., Abed F.M.: *The potential of LiDAR and UAV-photogrammetric data analysis to interpret archaeological sites: A case study of Chun Castle in South-West England*. ISPRS International Journal of Geo-Information, vol. 10(1), 2021, 41. https://doi.org/10.3390/ijgi10010041.

[31] Al-Manasir K., Fraser C.S.: *Registration of terrestrial laser scanner data using imagery*. The Photogrammetric Record, vol. 21(115), 2006, pp. 255–268. https://doi.org/10.1111/j.1477-9730.2006.00379.x.

[32] Theiler P.W., Schindler K.: *Automated registration of terrestrial laser scanner point clouds*. ISPRS Annals of the Photogrammetry, Remote Sensing and Spatial Information Sciences, vol. I-3, 2012, pp. 173–178. https://doi.org/10.5194/isprsannals-I-3-173-2012.

[33] Alsadik B., Gerke M., Vosselman G.: *Automated camera network design for 3D modeling of cultural heritage objects*. Journal of Cultural Heritage, vol. 14(6), 2013, pp. 515–526. https://doi.org/10.1016/j.culher.2012.11.007.

[34] Tonietto L., Gonzaga L. Jr., Veronez M.R., de Souza Kazmierczak C., Arnold D.C.M., da Costa C.A.: *New method for evaluating surface roughness parameters acquired by laser scanning*. Scientific Reports, vol. 9(1), 2019, 15038. https://doi.org/10.1038/s41598-019-51545-7.

[35] Wyjadłowski M., Muszyński Z., Kujawa P.: *Application of laser scanning to assess the roughness of the diaphragm wall for the estimation of earth pressure*. Sensors, vol. 21(21), 2021, 7275. https://doi.org/10.3390/s21217275.